Structural Engineering and Mechanics, Vol. 45, No. 1 (2013) 1-18
DOI: http://dx.doi.org/10.12989/sem.2013.45.1.001

Prediction of typhoon design wind speed and profile over complex terrain

W.F. Huang[*1,2] and Y.L. Xu[2a]

[1]*School of Civil Engineering, Hefei University of Technology, Anhui 230009, China*
[2]*The Hong Kong Polytechnic University, Kowloon, Hong Kong, China*

(Received May 4, 2011, Revised October 30, 2012, Accepted November 30, 2012)

Abstract. The typhoon wind characteristics designing for buildings or bridges located in complex terrain and typhoon prone region normally cannot be achieved by the very often few field measurement data, or by physical simulation in wind tunnel. This study proposes a numerical simulation procedure for predicting directional typhoon design wind speeds and profiles for sites over complex terrain by integrating typhoon wind field model, Monte Carlo simulation technique, CFD simulation and artificial neural networks (ANN). The site of Stonecutters Bridge in Hong Kong is chosen as a case study to examine the feasibility of the proposed numerical simulation procedure. Directional typhoon wind fields on the upstream of complex terrain are first generated by using typhoon wind field model together with Monte Carlo simulation method. Then, ANN for predicting directional typhoon wind field at the site are trained using representative directional typhoon wind fields for upstream and these at the site obtained from CFD simulation. Finally, based on the trained ANN model, thousands of directional typhoon wind fields for the site can be generated, and the directional design wind speeds by using extreme wind speed analysis and the directional averaged mean wind profiles can be produced for the site. The case study demonstrated that the proposed procedure is feasible and applicable, and that the effects of complex terrain on design typhoon wind speeds and wind profiles are significant.

Keywords: complex terrain; typhoon wind field; CFD simulation; surface roughness length; topography; neural network; design wind speed; wind profile

1. Introduction

Normally, strong winds have been associated with two types of wind in typhoon prone region. The first one is the nature wind and the other one is the typhoon, or say severe tropical cyclone, that is a large vortex of air movement and spirally in towards the center. To design buildings or bridges located in complex terrain and typhoon prone region, it is essential to know typhoon wind speed, direction, and profile, among other factors, over the complex terrain in the atmospheric boundary layer. At present, the required typhoon wind characteristics are acquired based on either field measurement data if there is a well-established weather station at the structure site or physical simulation in a boundary layer wind tunnel.

∗Corresponding author, Ph.D., E-mail: wfhuang@163.com
[a]Chair Professor, E-mail: ceylxu@polyu.edu.hk

However, in many cases there are no or only few field measurement data available at a structure site surrounded by complex terrain (Song *et al.* 2012). Therefore, very often the reliable estimation of typhoon wind field at the structure site could not be achieved. Topographic studies in wind tunnels could be performed to ascertain wind field at the site surrounded by complex terrain but upstream wind field should be simulated first. The upstream wind field is often simulated according to that specified in wind standars and codes, which is only an approximation to the real typhoon wind field (Chock and Cochran 2005). On the other hand, typhoon wind field models in conjunction with Monte Carlo simulation are often used to predict typhoon wind field and design wind speeds for a general terrain. This method was first suggested by Russell (1971) and developed by Tryggvason *et al*. (1976), Batts *et al*. (1980), Georgiou (1985), Vickery and Twisdale (1995), Vickery *et al*.(2009). Computational fluid dynamics (CFD) was also applied to evaluate wind fields over simple or complex terrain for given upstream wind fields, such as Bitsuamlak *et al*. (2004), Tamura *et al*. (2007), Lee *et al*. (2010), Wakes *et al*. (2010). The motivation of this study is thus raised from such a question: can we integrate typhoon wind field models, Monte Carlo simulation technique, and CFD to provide a prediction of typhoon wind fields and design wind speeds for a site surrounded by complex terrain?

In this regard, this paper first presents a refined typhoon wind field model. The refined typhoon wind field model together with the Monte Carlo simulation is then used to generate directional typhoon wind fields on the upstream of complex terrain with consideration of interaction between typhoon winds and terrain surface roughness. The representative directional upstream typhoon wind fields are then used as inputs and CFD is used as a tool to train artificial neural networks (ANN) model for predicting directional typhoon wind fields for the site over the complex terrain. Based on the trained ANN model, thousands of directional typhoon wind fields for the site can be generated. The extreme wind speed analysis can be then performed to determine the directional design wind speeds and the directional averaged mean wind profiles can be also produced for the site. Finally, the Stonecutters Bridge surrounded by complex terrain in Hong Kong is chosen as a case study to examine the feasibility of the proposed numerical simulation procedure for predicting typhoon wind fields over complex terrain.

2. Numerical simulation procedure

2.1 Refined typhoon wind field model

The refined typhoon wind field model considering the effect of temperature and the variation of atmospheric pressure with height (Huang and Xu 2011) is used in this study. The basic equations of the typhoon wind field model are given as follows

$$\frac{d\mathbf{v}_h}{dt} = -\frac{1}{\rho}\nabla_h p - f\mathbf{k}_h \times \mathbf{v}_h + \mathbf{F}_h \tag{1}$$

$$p = p_0(1 + gz / \theta c_p)^{c_p/R} \tag{2}$$

$$p_0 = p_{c0} + \Delta p_0 \exp[-(r_m / r)^B] \tag{3}$$

where h is the horizontal direction; $\mathbf{v}_h$ is the wind velocity in the horizontal plane; $\mathbf{k_h}$ is the unit

vector; $\boldsymbol{F}_h$ is the friction force in the horizontal direction; $\nabla_{\boldsymbol{h}}$ is the two-dimensional del operator; p is the atmospheric pressure; ρ is the air density; f is the Coriolis parameter; p_0 is the pressure at zero-plane; g is the gravitational constant; z is the height from ground surface; θ is the potential temperature; c_p is the heat capacity at constant pressure; R is the ideal gas constant; p_{c0} is the central pressure of a typhoon at zero-plane; Δp_0 is the central pressure difference at zero plane equal to p_{m0}-p_{c0}; p_{m0} is the ambient pressure (theoretically at infinite radius) at zero-plane; $r_{\max}$ is the radius to maximum wind speed; r is the radial distance from the typhoon center; and B is the Holland's radial pressure profile parameter, taking on values between 0.5 and 2.5.

If the typhoon makes landfall, a typhoon decay model shall be included in the basic equations of the typhoon wind field model (Vickery and Twisdale 1995). The basic equations of the typhoon wind field model can be solved by using the wind decomposition method (Ishihara *et al.* 1995).

2.2 Directional upstream typhoon wind fields of complex terrain

To simulate directional upstream typhoon wind fields with consideration of the interaction between typhoon winds and terrain surface roughness, the average and directional surface roughness length z_0 over the complex terrain are determined by using the Digital Elevation Model (DEM) information provided by the CGIAR (Consultative Group on International Agricultural Research) consortium together with land use information. The probability distributions of key typhoon parameters are established based on typhoon data for the area concerned. Based on the established probability distributions, the Monte Carlo simulation method is used to generate a set of key typhoon parameters for a typhoon at its initial position. This set of key typhoon parameters and the computed average surface roughness length z_0 are used as inputs to the refined typhoon wind field model to generate a typhoon wind field. For the typhoon wind field generated, the wind speed and direction can be identified for the structure site. If the directional surface roughness length identified is not the same as the average surface roughness length z_0, this set of key typhoon parameters and the directional surface roughness length shall be used to re-generate a typhoon wind field until the typhoon wind direction is consistent with the directional surface roughness length used. The wind speed and wind direction obtained by this way are regarded as one of the directional upstream typhoon wind field for the site over the complex terrain. Then, let this typhoon move at a one-hour time interval and repeat the above procedure to obtain another directional upstream typhoon wind field for the site until this typhoon disappears. Repeating the above steps for thousands of typhoons, a complete assembly of directional upstream typhoon wind fields can be obtained for the site over the complex terrain.

2.3 Representative directional typhoon wind fields at the site

The CFD simulation is used to determine representative directional typhoon wind fields at the site. In this regard, the topography of the complex terrain at the site shall be modeled with appropriate computational domain, meshes and boundary conditions. For a given wind direction, representative directional upstream typhoon wind fields are selected from all the generated upstream typhoon wind fields to make the problem manageable. By taking a representative upstream typhoon wind field as an inlet to the topographic model, the CFD simulation with the Reynolds-averaged Navier-Stokes (RANS) method is performed. The representative typhoon wind field at the site surrounded by the complex terrain can be obtained in the designated wind direction.

The governing equations of RANS method used in the CFD simulation for steady, incompressible flow are written as follows (Cheng *et al.* 2003)

$$\frac{\partial U_i}{\partial x_i} = 0 \tag{4}$$

$$\frac{\partial U_i U_j}{\partial x_j} = -\frac{1}{\rho}\frac{\partial P}{\partial x_i} + \frac{\partial}{\partial x_j}(\upsilon \frac{\partial U_i}{\partial x_j} - \overline{u_i' u_j'}) \tag{5}$$

where U_i and u_i' are the mean and fluctuating velocities in the x_i direction, respectively; ρ is the reference density; P is the mean pressure; υ is the viscosity coefficient. The presence of the Reynolds stress $\overline{u_i' u_j'}$ in Eq. (5) implies that the latter are not closed. Closure requires that some models be made in prescribing the Reynolds stresses in terms of the mean flow quantities. The most popular statistical turbulence closure model is the Boussinesq type of eddy viscosity approximation that assumes a linear relationship between the turbulence stresses and the mean velocity gradients

$$-\overline{u_i' u_j'} = v_t^* (\frac{\partial U_i}{\partial x_j} + \frac{\partial U_j}{\partial x_i}) - \frac{2}{3} k \delta_{ij} \tag{6}$$

where v_t^* is the kinematic eddy viscosity; $k \equiv \frac{1}{2}\overline{u_i' u_i'}$ is the turbulence kinetic energy.

In the standard k-ε model, v_t^* is determined as

$$v_t^* = C_\mu \frac{k^2}{\varepsilon} \tag{7}$$

where ε is the dissipation of turbulence kinetic energy. The standard model uses the following transport equations for k and ε

$$\frac{\partial (U_i k)}{\partial x_j} = \frac{\partial}{\partial x_j}\left[\left(\upsilon + \frac{v_t^*}{\sigma_k}\right)\frac{\partial k}{\partial x_j}\right] + v_t^*\left(\frac{\partial U_i}{\partial x_j} + \frac{\partial U_j}{\partial x_i}\right)\frac{\partial U_i}{\partial x_j} - \varepsilon \tag{8}$$

$$\frac{\partial (U_j \varepsilon)}{\partial x_j} = \frac{\partial}{\partial x_j}\left[\left(\upsilon + \frac{v_t^*}{\sigma_\varepsilon}\right)\frac{\partial \varepsilon}{\partial x_j}\right] + C_{\varepsilon 1}\frac{\varepsilon}{k}\left(\frac{\partial U_i}{\partial x_j} + \frac{\partial U_j}{\partial x_i}\right)\frac{\partial U_i}{\partial x_j} - C_{\varepsilon 2}\frac{\varepsilon^2}{k} \tag{9}$$

The equation contains five closure constants: namely C_μ, σ_k, σ_ε, $C_{\varepsilon 1}$, $C_{\varepsilon 2}$. The standard k-ε model employs values for constants that are determined by a comprehensive data fitting over a wide range of canonical turbulent flows

$$C_\mu = 0.09 \quad \sigma_k = 1.00 \quad \sigma_\varepsilon = 1.30 \quad C_{\varepsilon 1} = 1.44 \quad C_{\varepsilon 2} = 1.92 \tag{10}$$

The turbulent diffusion of k and ε in Eq. (8) and (9) are represented using a gradient diffusion hypothesis with the Prandtl numbers σ_k and σ_ε used to connect the eddy diffusivities of k and ε to the eddy viscosity v_t^*.

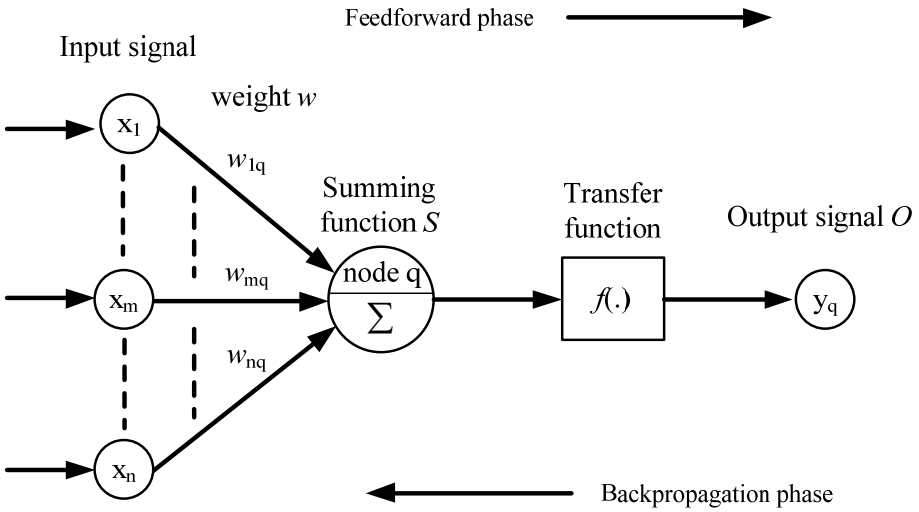

Fig. 1 A simple ANN using BPN method

2.4 Training NN model for the complex terrain around the site

The complete assembly of the representative upstream typhoon wind fields and the representative typhoon wind fields at the site is used as input and output data to train an ANN model for predicting directional typhoon wind fields (including wind speed, wind direction and wind profile) at the site over complex terrain. The backpropagation network (BPN) method (Rumelhart *et al.* 1986) is used in this study to train the ANN model. During the training, the ANN model learns how to map the input parameters from the representative directional upstream typhoon wind fields into the output parameters from the representative directional typhoon wind fields at the site through an iterative process that involves optimization and other mathematical operations.

As a simple example, an elementary BPN neuron with n inputs and weighted connections is shown in Fig. 1. The training of this simple ANN involves two phases: feedforward phase and backpropagation phase. In the feedforward phase, each input signal x_i (i=1,…, n) is weighted with an approximate weight w, and the products are then summed up at the neuron of the network. This summation S of the weighted inputs at the neuron is modified by a transfer function f, thereby generating an output signal O. In practice, a continuous, non-linear logistic or sigmoid transfer function is commonly used because it meets the differentiability requirement of the backpropagation algorithm given by

$$f(S) = \frac{1}{1+e^{-aS}} \tag{11}$$

where a is the slope parameter of the sigmoid function; and $f(\ )$ is the transfer function.

The output signal O is then compared with the designated output, from which an error signal is obtained and the backpropagation phase is activated. The error signal is transmitted backward to the neuron of the network. Based on the error signal received, the connection weights w for the network are updated. A new output signal O is then obtained by using the new weights w, and a

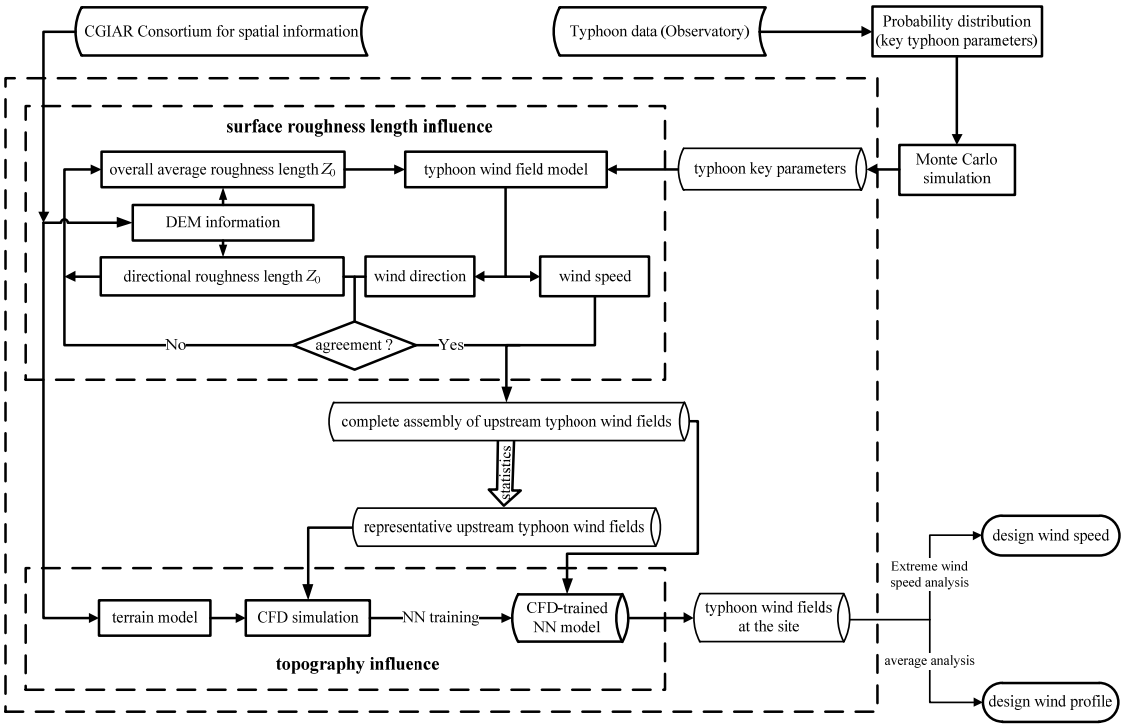

Fig. 2 Numerical simulation procedure for predicting directional design wind speeds and wind profiles for the site over complex terrain

new error signal is calculated. The above procedure is repeated until the error signal is small enough to satisfy the preset criterion. The training is discontinued when all the training data are used up.

Once the ANN model is trained, the ANN model shall be then validated by using a few new sets of input and output data to make sure the ANN model is of the proper internal relationship. Finally, by using the validated ANN model and all the directional upstream typhoon wind fields, a complete assembly of directional typhoon wind fields at the site surrounded by the complex terrain can be obtained for the estimation of directional design wind speeds for a given return period and averaged wind profiles for design.

2.5 Directional design wind speeds and wind profiles at the site

Based on the assembly of directional typhoon wind fields at the site and the annual occurrence rate of typhoons in the area of interest, a series of directional annual maximum wind speeds at the site over the complex terrain can be found for a given height above the sea level. By performing an extreme wind speed analysis, the directional design wind speeds at the site can be determined for a given return period. By averaging mean wind speed profiles for a given wind direction, the directional design mean wind profile can be produced. The flow chart of the entire numerical simulation procedure for predicting directional design wind speeds and wind profiles for the site over the complex terrain is displayed in Fig. 2.

3. Case study

The site of the Stonecutters Bridge in Hong Kong is chosen as a case study. This is because this bridge is an important structure (the second longest cable-stayed bridge in the world) and the bridge site is surrounded by complex terrain, as indicated by Fig. 3.

3.1 Surface roughness lengths and directional upstream typhoon wind fields

To obtain directional upstream typhoon wind fields for the Stonecutters Bridge, the average and directional surface roughness lengths for the complex terrain around the bridge site shall be determined. The value of the average and directional surface roughness lengths can be estimated by using the following formula, which can be represented as

$$z_0 = \frac{\sum_{i=1}^{N} z_{0i} A_i}{A} \tag{12}$$

where z_0 is the average or directional surface roughness length; z_{oi} and A_i are the surface roughness length and area occupied by the surface roughness element i; A is the total area of complex terrain that the N elements occupy.

In this regard, the circular area taking the bridge as a center with a proper radius shall be considered (see Fig. 4). The circular area is further divided in consideration of 16 wind directions. Then, by using the DEM information and the land use information in Hong Kong, the surface roughness length z_{oi} and area A_i for each surface roughness element i within the circular area can be determined. Accordingly, by using Eq. (12), the average and directional surface roughness

Fig. 3 Location of Stonecutters Bridge and its surrounding topography

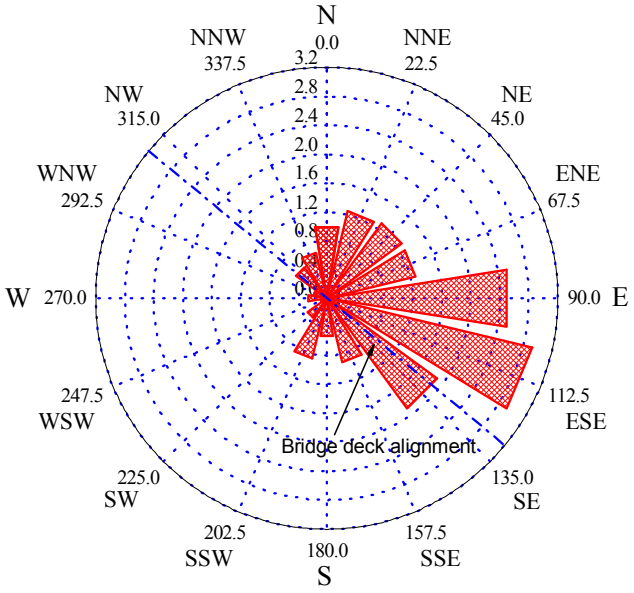

Fig. 4 Directional surface roughness length around the bridge

Table 1 Directional surface roughness length z_0 for the complex terrain around Stonecutters Bridge

Sector	True Azimuth (degree)	z_0 (m)	Sector	True Azimuth (degree)	z_0 (m)
N	0	0.992	S	180	0.533
NNE	22.5	1.245	SSW	202.5	0.861
NE	45	1.282	SW	225	0.334
ENE	67.5	1.262	WSW	247.5	0.087
E	90	2.515	W	270	0.258
ESE	112.5	2.913	WNW	292.5	0.192
SE	135	1.882	NW	315	0.532
SSE	157.5	0.909	NNW	337.5	0.649

length z_0 around the bridge can be estimated for different radiuses (5 km, 10 km, 20 km, 30 km) and resolutions (30 m, 60 m, 90 m). By analyzing the obtained results and in consideration of the subsequent CFD simulation, the average and directional surface roughness lengths for the area with a radius of 30 km and a resolution of 30m are used for the typhoon simulation and given in Fig. 4 and Table 1. The average surface roughness length z_0 for the entire area is 1.027 m. It can be seen that the maximum directional surface roughness length z_0 is about 2.9 m from E and ESE the far field effect is induced by buildings in Kowloon and Hong Kong Island. The minimum directional surface roughness length z_0 is about 0.09 m from around WSW direction which is effected by the open sea. In summary, the directional surface roughness length z_0 can represent the spatial surface roughness element distribution for the complex terrain around Stonecutters Bridge within this circular area and can be used for obtaining directional upstream typhoon wind field.

By using the Monte Carlo simulation method, the refined typhoon wind field model, the

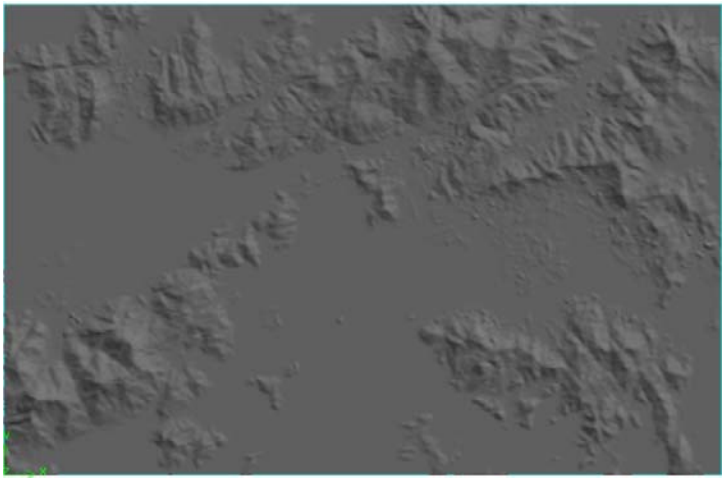

Fig. 5 Top view of topographic model

probability distributions of key typhoon parameters (Xu and Huang 2009), the average and directional surface roughness lengths, and following the procedure described in section 2.2, a complete assembly of directional upstream typhoon wind fields around the bridge are obtained for the subsequent CFD simulation.

3.2 Topographic model and representative typhoon wind fields at the site

The topographic model used for CFD simulation is set up based on the DEM information provided by the CGIAR Consortium. The area of computational domain with the bridge site as a center is 38 km in East-West and 25 km in North-South. Because the highest mountain within the computational domain is 957 m high, the computational domain in the vertical direction is set as 4 km so that the flow field can be fully developed. Fig. 5 shows the top view of the topographic model around the Stonecutters Bridge, and Fig. 6 displays the mesh grid for the topographic model. In horizontal level, the topographic model is meshed with 200 (East-West) × 100 (North-South) parts. Vertical level is divided into 80 parts, and an expansion factor 1.05 is imposed (Maurizi *et al.* 1998). A total of 1.65 million nodes are used for CFD simulation.

For a given direction, the surface of the topographic model is modeled as a non-slip wall boundary. The flow inlet boundary is set as wind inlet profile with representative directional upstream wind field while the outlet boundary is specified as fully developed outflow boundary conditions. The side and top boundaries are all defined in such a way that the gradients of flow variables (including velocity and pressure) normal to those boundary faces are zero. Present simulations have been performed with Fluent, and a general-purpose code for fluid dynamic simulations produced by Fluent Inc. The Reynolds-averaged Navier-Stokes (RANS) method is applied to perform CFD simulation to obtain representative typhoon wind fields at the bridge site, in which the finite volume method and the first order upwind scheme for spatial discretization were used and the SIMPLEC method was adopted to solve velocity and pressure simultaneously. The simulation is discontinued until residuals for all variables reach 10^{-3} accuracy and keep as constant.

For a given wind direction, representative directional upstream typhoon wind fields are selected from all the generated upstream typhoon wind fields in this direction. By taking a representative

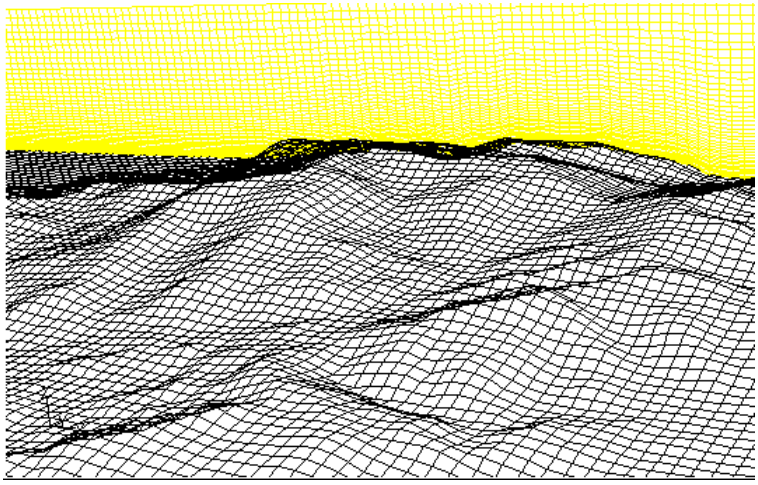

Fig. 6 Mesh grid of topographic model

upstream typhoon wind field as an inlet to the topographic model, the CFD simulation is performed. The representative typhoon wind fields at the site surrounded by the complex terrain can be obtained. Repeating the above steps for all the wind directions, a complete assembly of the representative upstream typhoon wind fields and the representative typhoon wind fields at the bridge site are obtained. They are subsequently used as input and output data to train an ANN model for typhoon wind fields at the site.

3.3 Establishment of ANN model

In theory, for thousands of upstream typhoon wind field for the complex terrain for all the wind directions around the bridge site, a complete assembly of the directional typhoon wind field at the bridge site can be obtained by using CFD simulation with the topographic model. However, thousands of CFD computational cost during this simulation process will be tremendous. Therefore, this process is possible in theory, but it is difficulty in practical use. Instead of using CFD simulation directly, a trained ANN model using representative directional upstream typhoon wind fields and representative typhoon wind fields at Stonecutters Bridge obtained from CFD simulation is used to solve this problem.

The ANN model architecture for wind speed and wind direction with the input and output variables is shown in Fig. 7 which consists of one hidden layer with an input layer and output layer. The input variables for ANN model are the upstream typhoon wind speed $v(z)$ and wind direction $\theta(z)$ at height z from ground surface. The output parameters for ANN model are wind speed $v'(z)$ or wind direction $\theta'(z)$ at the height z at the bridge site.

The input training data for input variables are the representative direction upstream typhoon wind fields obtained from the complete assembly of directional upstream typhoon wind field. For any given direction, all upstream typhoon wind speed profiles are fitted by using power law relationship for convenience, and the 10 m height wind speed v_{10} and power law exponent index α for all upstream typhoon wind speed profiles can be determined. Furthermore, by supposing the power law exponent index α for upstream typhoon wind profiles at any given direction obeys the normal distribution, the power law exponent index α interval with confidence level 0.95 for the

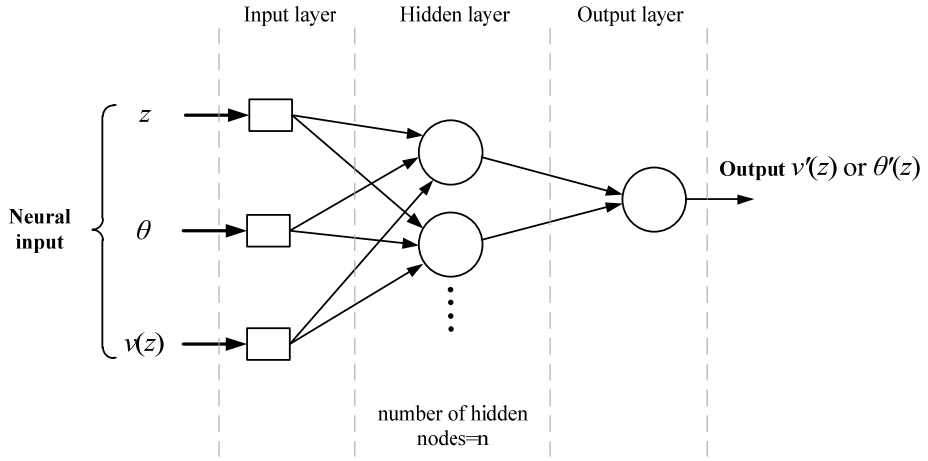

Fig. 7 ANN model architectures with input and output parameters for wind speed and wind direction; circles represent processing elements, squares represent non-processing elements

Table 2 Statistical results of power law exponent index α for upstream typhoon wind field at different directions around Stonecutters Bridge

Sector	Mean value	Standard deviation	Confidence interval	Sector	Mean value	Standard deviation	Confidence interval
N	0.142	0.039	[0.07 0.22]	S	0.114	0.039	[0.04 0.19]
NNE	0.149	0.040	[0.07 0.23]	SSW	0.129	0.039	[0.05 0.21]
NE	0.149	0.038	[0.07 0.22]	SW	0.098	0.032	[0.04 0.16]
ENE	0.154	0.045	[0.07 0.24]	WSW	0.071	0.027	[0.02 0.12]
E	0.217	0.048	[0.12 0.31]	W	0.075	0.026	[0.02 0.13]
ESE	0.218	0.059	[0.10 0.33]	WNW	0.084	0.026	[0.03 0.13]
SE	0.161	0.054	[0.06 0.27]	NW	0.107	0.036	[0.04 0.18]
SSE	0.134	0.052	[0.03 0.24]	NNW	0.128	0.036	[0.06 0.20]

complete assembly of directional upstream typhoon wind field at different directions can be determined, as given in Table 2. In consideration of different 10m height wind speed v_{10} and the power law exponent index α results shown in Table 2, the representative upstream typhoon wind fields at different directions used as the input data for training ANN model are determined, which is shown in Table 3. Then, by taking the representative upstream typhoon wind field as the wind inlet profile to the topographic model, CFD simulations are performed and the representative typhoon wind fields at the bridge site used as the output training data for ANN model can be obtained. For example, for representative upstream typhoon wind field coming from N direction with different 10 m height wind speeds v_{10} (10 m/s, 30 m/s, 50 m/s) and power law exponent index α 0.22, the representative typhoon wind field at the bridge site obtained from CFD simulation are shown in Fig. 8.

To train the ANN model, upstream typhoon wind fields and typhoon wind fields at the bridge site are selected pair by pair. They are then normalized by its maximum value so that they vary between 0 and 1. The normalized pairs are used as input and output parameters to train the ANN model. By trial and error, the neuron numbers in the hidden layer are set as 25. The learning

Table 3 Representative upstream typhoon wind fields used as input data for the ANN model

Sector	Power law exponent α	wind speed (m/s)	Sector	Power law exponent α	wind speed (m/s)
N	0.07,0.16,0.22	10,30,50	S	0.04,0.12,0.19	10,30,50
NNE	0.07,0.16,0.23	10,30,50	SSW	0.05,0.12,0.21	10,30,50
NE	0.07,0.16,0.22	10,30,50	SW	0.04,0.12,0.16	10,30,50
ENE	0.12,0.16,0.24	10,30,50	WSW	0.02,0.08,0.13	10,30,50
E	0.12,0.22,0.31	10,30,50	W	0.02,0.08,0.13	10,30,50
ESE	0.10,0.22,0.33	10,30,50	WNW	0.03,0.08,0.13	10,30,50
SE	0.06,0.16,0.27	10,30,50	NW	0.04,0.12,0.18	10,30,50
SSE	0.03,0.16,0.24	10,30,50	NNW	0.06,0.12,0.20	10,30,50

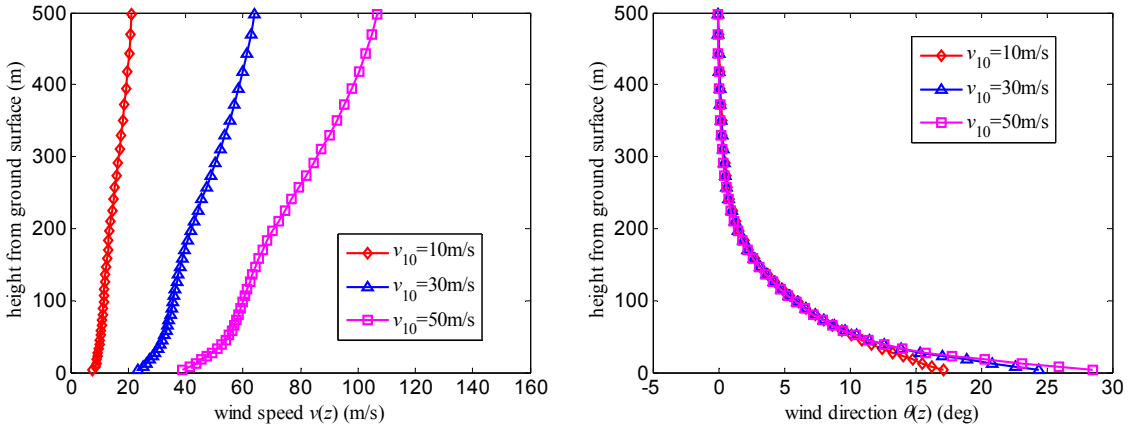

(a) Wind speed profile (b) Wind direction profile

Fig. 8 ANN model output training data for upstream typhoon wind field coming from N direction with exponent 0.22

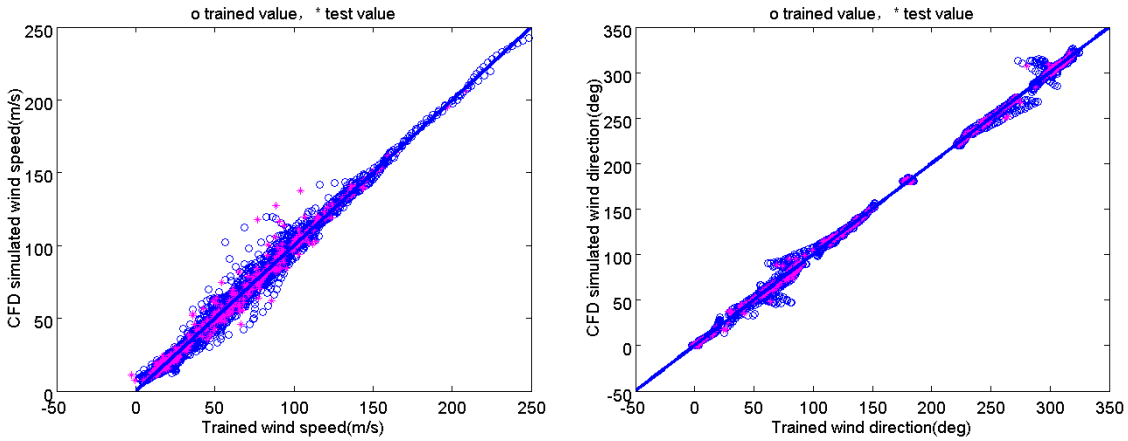

(a) Wind speed (b) Wind direction

Fig. 9 Scatter diagram between target value and ANN output value

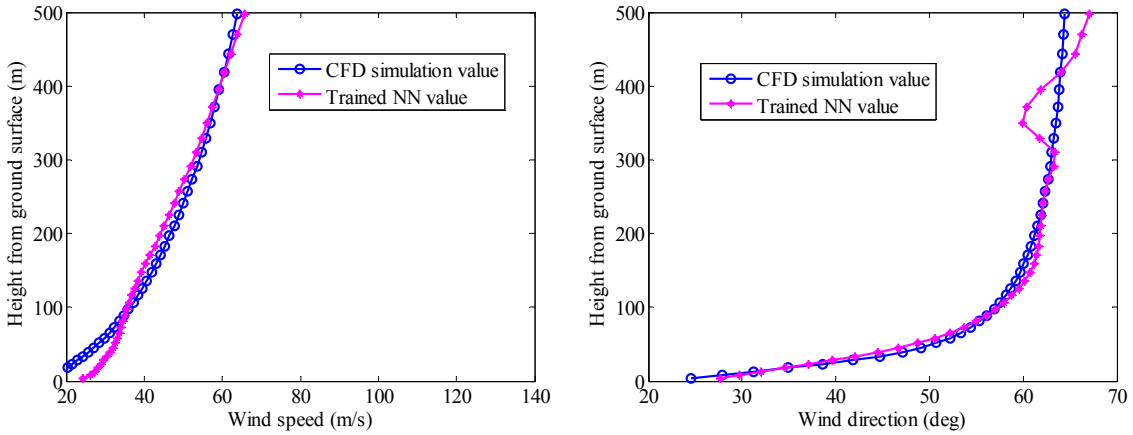

(a) Wind speed (b) Wind direction

Fig. 10 Scatter diagram between trained ANN data and CFD simulation data for upstream typhoon wind field coming from ENE direction

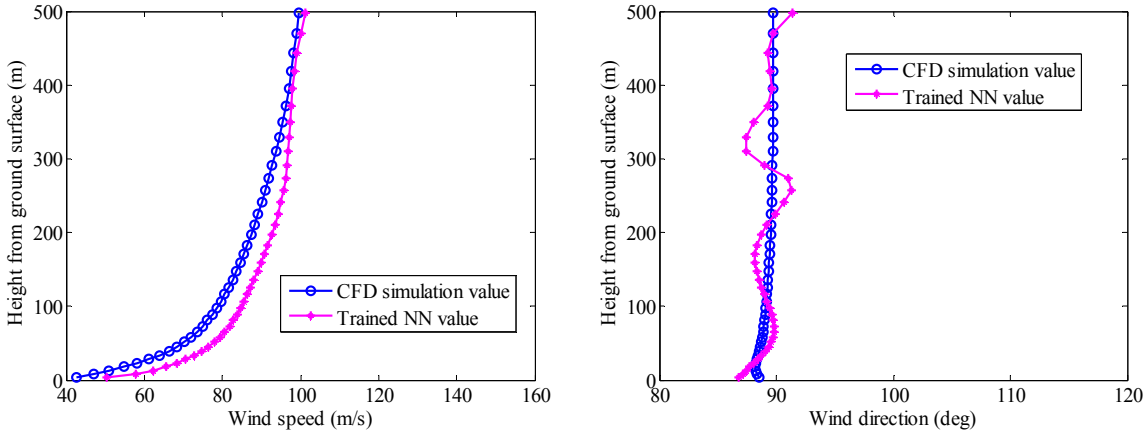

(a) Wind speed (b) Wind direction

Fig. 11 Scatter diagram between trained ANN data and CFD simulation data for upstream typhoon wind field coming from E direction

rate parameter is kept constant with 0.001. The maximum training iterative step is set 2000. The training of the network is carried out until the root mean square error of the network is smaller than 0.0001. The scatter diagrams for wind speed and direction between target values obtained from CFD simulation and output values obtained from the trained NN model have been plotted in Fig. 9. The diagram shows that the checking of training data is with small error, about 8% mean percentage error for wind speed and 3 degree mean absolute error for wind direction.

After the ANN model is trained, the trained ANN model is tested in reproducing the typhoon wind field at bridge site for upstream typhoon wind fields coming from ENE direction with reference wind speed v_{10} of 30 m/s and power law exponent index 0.22, E direction with reference wind speed v_{10} of 30 m/s and power law exponent index 0.30 to confirm the efficiency of using the trained ANN model to predict typhoon wind speed and wind direction at the bridge site. The

scatter diagrams between the trained ANN model value and the CFD simulation value for the upstream typhoon wind field coming from ENE direction and E direction are shown in Fig. 10 and Fig. 11. It can be known that, for wind speed, the checking of training data is with small mean percentage error, about 9% and 8%. For wind direction, the checking of training data is also with small mean absolute error, about 1.2 degree and 0.8 degree. All test runs have shown that the trained ANN model can be used effectively to predict the typhoon wind field at the bridge site.

3.4 Directional design wind speeds and wind profiles

By using the trained ANN model, the directional typhoon wind fields at the bridge site are computed based on the directional upstream typhoon wind fields generated by 3000 typhoons. By taking 10m as a reference height, a series of annual maximum wind speeds at 10m high in each of 36 direction sectors are obtained based on the Poisson distribution of annual occurrence rate of typhoons. Then, by using the Type I extreme distribution, the directional design wind speed of a 50 year return period is determined for the bridge site in each of 36 directional sectors, and the results are shown in Fig. 12 and Table 4. It can be seen that the minimum design wind speed of about 23 m/s at 10m height occurs mainly from N direction to ENE direction due to the mountains. The maximum design wind speed comes from S direction of about 38m/s due to open sea.

Furthermore, the mean wind speeds and wind directions at different heights are also simulated for each typhoon at the bridge site by using the trained ANN model, from which mean wind profiles can be obtained. By averaging all the mean wind profiles for a given wind direction, the directional mean wind profile at the bridge site surrounded by the complex terrain can be obtained as the design directional wind speed profile, which is shown in Fig. 13. The comparison of the design wind speed profile in 40^o 180^o and 270^o direction at the bridge site with the corresponding averaged upstream mean wind profile in the same direction are shown in Figs. 14-16. Mount chain modeled in here is mostly in west-east direction. When the wind blows from 40^o direction, with a view of relation between topographical configuration and wind speed, the Stonecutters Bridge is located in the down direction of hills which leads a small wind speed value. In addition, since the

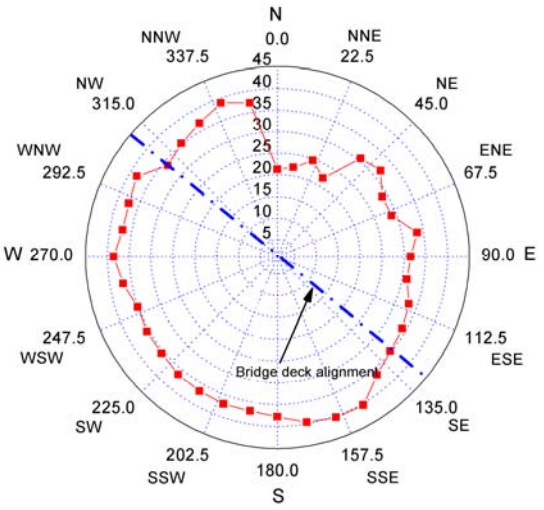

Fig. 12 Directional design wind speeds at the bridge site at 10 m high

Table 4 Directional design wind speeds at the bridge site at 10 m high

True Azimuth (degree)	Wind speed (m/s)	True Azimuth (degree)	Wind speed (m/s)	True Azimuth (degree)	Wind speed (m/s)
0	22.8	120	33.7	240	34.4
10	22.5	130	33.9	250	34.3
20	24.8	140	35.4	260	36.4
30	22.2	150	39.1	270	37.1
40	29.9	160	38.9	280	35.7
50	31.8	170	38.4	290	36.6
60	28.9	180	36.9	300	37.3
70	28.4	190	35.9	310	31.2
80	32.8	200	35.9	320	33.1
90	31.4	210	35.6	330	34.6
100	31.8	220	35.4	340	36.9
110	33.0	230	34.4	350	35.4

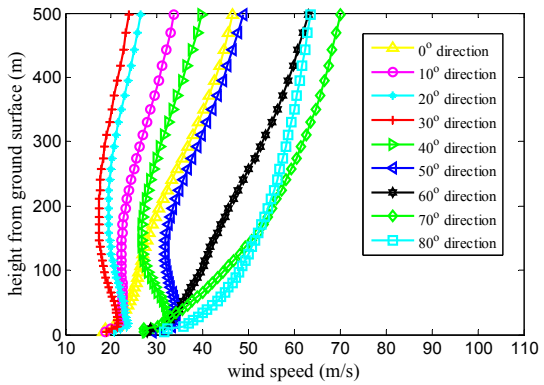

(a) wind profile from N to ENE direction

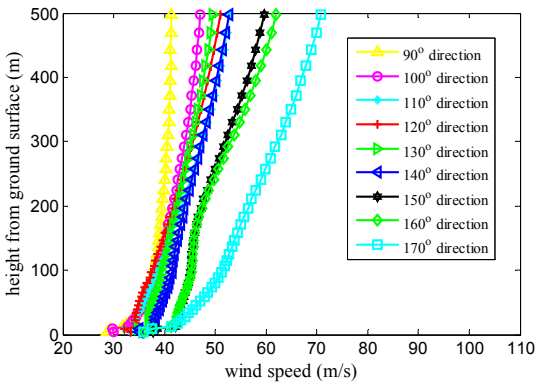

(b) wind profile from E to SSE direction

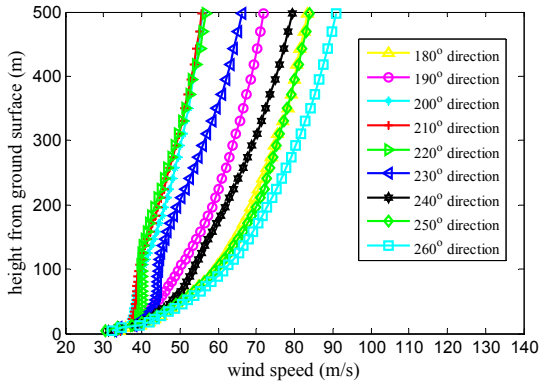

(c) wind profile from S to WSW direction

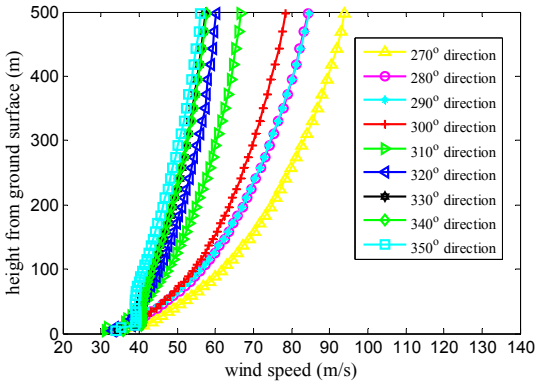

(d) wind profile from W to NNW direction

Fig. 13 Directional design wind profiles at the bridge site

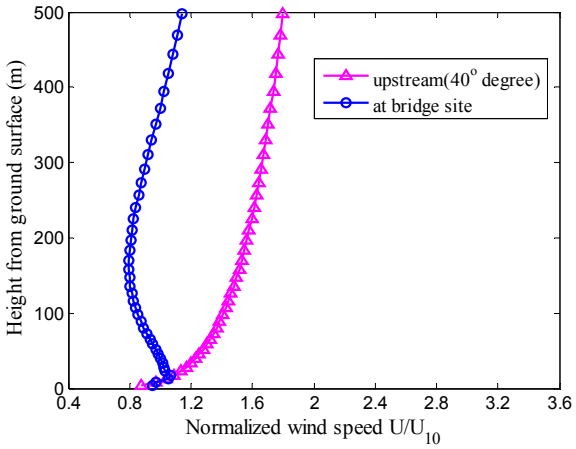

Fig. 14 Comparison of directional design wind speeds for upstream and at the bridge site (40° direction)

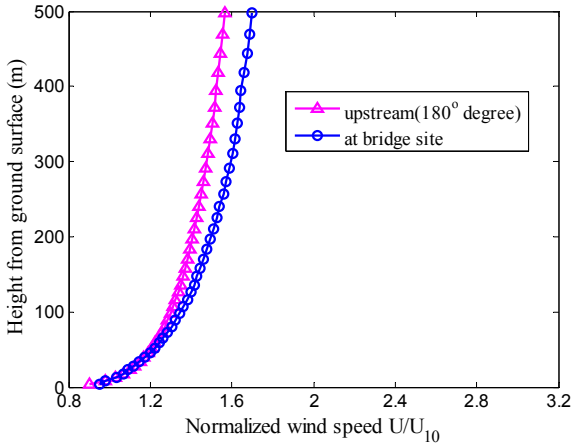

Fig. 15 Comparison of directional design wind speeds for upstream and at the bridge site (180° direction)

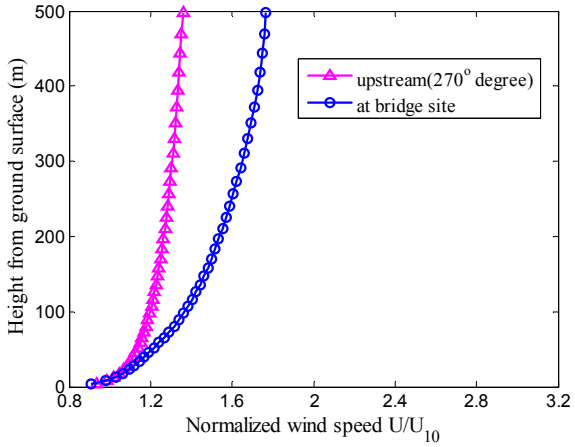

Fig.16 Comparison of directional design wind speeds for upstream and at the bridge site (270° direction)

heights of all these hills have a value larger than 500 m, this will lead that the wind speed is smaller than the averaged upstream wind speed up to 500 m. In lower height especially near ground surface, the wind speed has a relatively small change under the influence of incoming flow component from E direction which gives a flow acceleration effect to wind speed.

When the wind blows from 180^o direction, the mean wind profile mainly affects by the extensive open sea and there is a very little valley speed up effect formed by Hong Kong Island and Lantau Island on the two sides, so the mean wind profile has a little variation compared with the averaged upstream mean wind profile in this direction. When the wind blows from 270^o direction, it can be seen that there exist a relatively large speed up effect between mount chain in west-east direction and Lantau Island in this direction, so the mean wind profile has a relatively larger value than the averaged upstream mean wind profile in this direction. In summary, it can be seen that the effect of complex terrain around Stonecutters Bridge on mean wind speed profile is significant.

4. Conclusions

A numerical simulation procedure for predicting directional typhoon wind fields over complex terrain has been proposed in this study. The proposed procedure was then applied to the complex terrain around the Stonecutters Bridge in Hong Kong, which is located in a typhoon prone region, as a case study to examine its feasibility and applicability. In the case study, the average and directional surface roughness lengths for the bridge site were determined based on the DEM information and land use information, and thousands of directional upstream typhoon wind fields for the bridge site were generated based on statistical typhoon data and using the refined typhoon wind field model. The topographic model for the bridge site within the complex terrain was then established, and the representative directional typhoon wind fields at the bridge site were obtained through a series of CFD simulations. The ANN model for predicting directional typhoon wind fields at the bridge site was finally established and used to determine the directional design typhoon wind speeds and wind profiles for the Stonecutters Bridge. The case study demonstrated that the proposed procedure is feasible and applicable, and that the effects of complex terrain on design typhoon wind speeds and wind profiles are significant.

Acknowledgments

The work described in this paper was financially supported by the Natural Science Foundation of China through its key program (NSFC 50830203) and by the Hong Kong Polytechnic University through its Niche Area Programs (PolyU 1-BB20 and 1-BB68), and by the Fundamental Research Funds for the Central Universities (Hefei University of Technology).

References

Batts, M.E., Simiu, E. and Russell, L.R (1980), "Hurricane wind speeds in the United States", *Journal of the Structural Division*, **106**(10), 2001-2016.

Bitsuamlak, G.T., Stathopoulos T. and Bedard, C. (2004), "Numerical simulation of wind flow over

complex terrain: review", *Journal of Aerospace Engineering*, **17**(4), 135-145.
Cheng, Y., Lien, F.S., Yee, E. and Sinclair, R. (2003), "A comparison of large eddy simulations with a standard *k-ε* Reynolds-averaged Navier-Stokes model for the prediction of a fully developed turbulent flow over a matrix of cubes", *Journal of Wind Engineering and Industrial Aerodynamics*, **91**, 1301-1328.
Chock, G.Y.K. and Cochran, L. (2005), "Modeling of topographic wind speed effects in Hawaii", *Journal of Wind Engineering and Industrial Aerodynamics*, **93**, 623-638.
Georgiou, P.N. (1985), *Design wind speeds in tropical cyclone-prone regions*, PhD Thesis, University of Western Ontario, London, Ontario, Canada.
Huang, W.F. and Xu, Y.L. (2012), "A refined model for typhoon wind field simulation in boundary layer", *Advances in Structural Engineering*, **15**(1), 77-89.
Lee, M., Lee, S.H., Hur, M. and Choi, C.K. (2010), "A numerical simulation of flow field in a wind farm on complex terrain", *Wind and Structures*, **13**(4), 375-388.
Xu, Y.L., Huang and W.F. (2009), Typhoon wind simulation and design wind speed, *Proceedings of the 6th International Advanced School on Wind Engineering*, Beijing, 323-345.
Ishihara, T., Matsui, M. and Hibi, K. (1995), "An analytical model for simulation of the wind field in a typhoon boundary layer", *Journal of Wind Engineering and Industrial Aerodynamics*, **56**, 291-310.
Rumelhart, D.E., Hinton, G.E. and Williams, R.J. (1986), *Learning internal representation by error propagation, in Rumelhart, D.E. et al. eds., Parallel Distributed Processing*, MIT Press, Cambridge, MA.
Russell, L.R. (1971), "Probability distributions for hurricane effects", *Journal of the Waterways, Harbors and Coastal Engineering Division*, **97**(1), 139-154.
Song L., Li Q.S., Chen W., Qin P., Huang H. and He Y.C. (2012), "Wind characteristics of a strong typhoon in marine surface boundary layer", *Journal of Wind and Structures*, **15**(1), 1-15.
Tamura, T., Okuno, A. and Sugio, Y. (2007), "LES analysis of turbulent boundary layer over 3D steep hill covered with vegetation", *Journal of Wind Engineering and Industrial Aerodynamics*, **95**, 1463-1475.
Vickery, P.J. and Twisdale, L.A. (1995), "Wind field and filling models for hurricane wind speed predictions", *Journal of Structural Engineering*, **121**(11), 1700-1709.
Vickery, P.J. (2009), "U.S. hurricane wind speed risk and uncertainty", *Journal of Structural Engineering*, **135**(3), 301-320.
Wakes, S.J., Maegli, T., Dickinson, K.J. and Hilton, M.J. (2010), "Numerical simulation of wind flow over complex terrain", *Environmental Modeling & Software*, **25**, 237-247.